Ni_3AlB: A bridge between superconductivity and ferromagnetism

Izumi Hase*
Nanoelectronics Research Institute AIST, Tsukuba, 305-8568, Japan
(Received 12 December 2003; revised manuscript received 26 April 2004; published 30 July 2004)

The electronic energy band structures of anti-perovskite-type intermetallic compound Ni_3AlB have been calculated within the local-density approximation Ferromagnetism does not appear even though the lattice is more expanded than nondoped Ni_3Al. We found that the Fermi surfaces of Ni_3AlB resemble those of $MgCNi_3$, which is known to be a superconductor with $T_c=8$ K, and a good candidate of unconventional superconductor.

DOI: 10.1103/PhysRevB.70.033105 PACS number(s): 71.20.Lp, 74.25.Jb, 71.18.+y

Recently discovered $MgCNi_3$ (Ref. 1) has stimulated intensive studies, because it contains large proportion of Ni, which is a typical ferromagnetic element. The superconductivity near ferromagnetism is realized in such as $ZrZn_2$ ($T_c \sim 0.3$ K),[2] UGe_2 ($T_c \sim 1$ K),[3] and Sr_2RuO_4 ($T_c \sim 1.5$ K),[4] and are now regarded as unconventional superconductivity with spin-triplet pairing. Like these compounds, $MgCNi_3$ is near ferromagnetism. Band calculation suggests that only 12% substitution of Na for Mg give rise to ferromagnetism.[5] $MgCNi_3$ has about an order of magnitude higher T_c(=8.5 K) than these compounds. Hence it is very important that whether $MgCNi_3$ has the same mechanism of superconductivity as these compounds or not. However, the mechanism of superconductivity in $MgCNi_3$ is still unclear. Tunneling spectroscopy indicates a zero-bias anomaly (clear peak [6] or a very high conductance [7]), which suggests a finite density of states at the Fermi level in the superconducting state (i.e, literally a gapless state). On the other hand, superconductivity is found even in the polycrystalline sample,[1] contrary to the case of $ZrZn_2$, UGe_2, and Sr_2RuO_4. Moreover, the nuclear magnetic resonance (NMR) experiment shows a clear Hebel-Slichter peak in ^{13}C relaxation rate.[8] These results suggest, literally, that the symmetry of the superconducting gap is simple *s*-wave. Band structure calculation shows that electron-phonon interaction in $MgCNi_3$ is moderately strong,[9] and suggests that $MgCNi_3$ is in the strong-coupling regime.

On the other hand, Ni_3Al has attracted much attention because of its unique mechanical properties in the past three decades. Moreover, this compound shows a typical itinerant weak ferromagnetism, and because of its simple crystal structure, extensive theoretical studies are developed. It is noteworthy that the above-mentioned $ZrZn_2$ also shows a typical itinerant weak ferromagnetism. Recently, in order to realize strong ferromagnetism by lattice expansion, several forms of chemical doping were tried. Contrary to the simple expectation, while all of the Ni_3AlX_y (X=B,C,N,H) compounds show a lattice expansion, none of them show ferromagnetism.[10] However, this result invokes another interest: Ni_3Al is a weak ferromagnet, and so is $ZrZn_2$. Then how about Ni_3AlX_y, in which the magnetic moment is depressed, but could it be superconducting or not? Moreover, stoichiometric Ni_3AlX has the same crystal structure as $MgCNi_3$, and especially Ni_3AlB is isoelectronic with $MgCNi_3$. In this paper we performed a band calculation of Ni_3AlB, and report

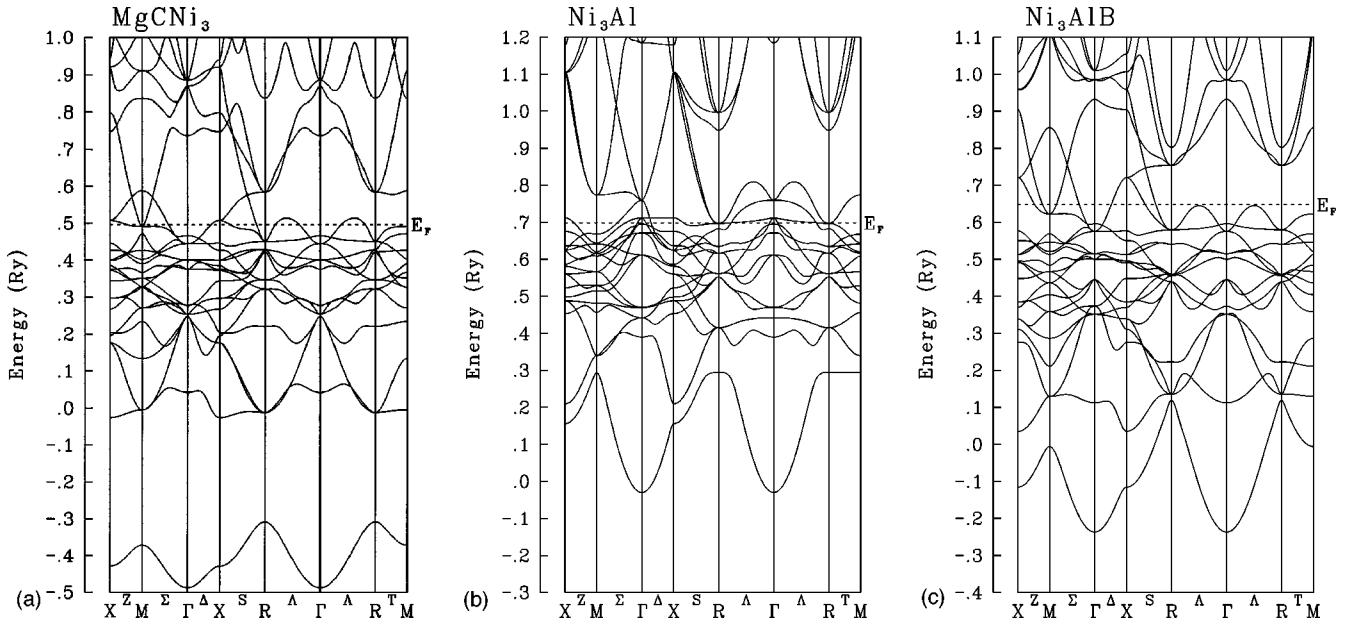

FIG. 1. Band structure of (a) $MgCNi_3$, (b) Ni_3AlB, and (c) Ni_3Al.

that the electronic structure of Ni_3AlB has many common features with $MgCNi_3$. Thus Ni_3AlB can be a crucial link between weak ferromagnetism and superconductivity.

The scheme we used in our calculations is the standard full-potential augmented plane wave (FLAPW) method. The present energy-band calculation was performed using the computer code KANSAI-94 and TSPACE.[11] For the exchange-correlation potential we adopted the local-density approximation (LDA), according to Gunnarson and Lundqvist.[12] The lattice constant a is systematically varied and the corresponding total energy is calculated. Muffin-tin (MT) radii are set to $0.41a$ for Al/Mg, $0.21a$ for B/C, and $0.29a$ for Ni, where a denotes the lattice constant. The absolute value of the total energy slightly depends on the MT radii but the equibilium a and the bulk modulus are hardly changed. Plane wave basis functions are used with a wave vector $|\mathbf{k}+\mathbf{G}|<K_{\max}=3.60(2\pi/a)$, where $\mathbf{k}$ is a wave vector in the Brillouin zone and $\mathbf{G}$ is a reciprocal-lattice vector, and resulted in about 400 LAPWs. The self-consistent potentials are calculated at 56 $\mathbf{k}$-points in the irreducible Brillouin zone (IBZ, 1/48th of the BZ). The density of states (DOS) are deduced from the eigenstates at 165 points in the same IBZ by the ordinary tetrahedron method. The optimized lattice parameter a is 3.778 Å for $MgCNi_3$, 3.765 Å for Ni_3AlB, and 3.526 Å for Ni_3Al. The calculated bulk modulus B using a Murnaghan equation of state is 210 GPa for $MgCNi_3$, 241 GPa for Ni_3AlB, and 216 GPa for Ni_3Al. These values are in good agreement with calculations for Ni_3Al,[13,14] but significantly different from the calculated value for $MgCNi_3$ by Hayward *et al.*,[15] who used the LMTO technique.

The energy band dispersions of $MgCNi_3$, Ni_3AlB, and Ni_3Al are shown in Fig. 1 along the principal symmetry axes in the Brillouin zone. Obtained band structures of $MgCNi_3$ and Ni_3Al are similar to previous calculations.[5,9,13–18] As expected, the overall shape of the bands in the valence region resembles between $MgCNi_3$ and Ni_3AlB. The main difference is the width of the valence band. The C-*s* bands in $MgCNi_3$ are far from the Ni-*d* bands and are "inactive," but the B-*s* bands in Ni_3AlB nearly touches the Ni-*d* and B-*p* manifold at the *R*-point. Moreover, the hybridization between Ni-*d* and B-*p* orbitals is stronger than that of Ni-*d* and *C*-*p* orbitals, and thus the valence bandwidth of Ni_3AlB is larger than that of $MgCNi_3$ as a whole. We present the total and partial density of states (MT-sphere-projected DOS) in Fig. 2. The Ni-*d* bandwidth is roughly estimated as 0.20 Ry in $MgCNi_3$ and 0.26 Ry in Ni_3AlB. The role of the B atom is crucial: Al-*p* orbitals play an important role in Ni_3Al, but in the presence of the B-atom, the energy of the extended Al-*p* orbitals goes up and becomes almost inactive near the Fermi level. The characteristic van-Hove singularity (vHS) peak just below the Fermi level (E_F) is smeared out in $NiAl_3$, probably due to the hybridization of Al-*p* bands. Strong *p*-*d* hybridization in Ni_3Al and its boron-doping effect is also discussed by Sun *et al.*[19] for $Ni_3AlB_{1/3}$.

Total and partial density of states (MT-sphere-projected DOS) of $MgCNi_3$, Ni_3AlB, and Ni_3Al are shown in Fig. 2. The DOS at the Fermi level $D(E_F)$ is 78 [states/Ry] in $MgCNi_3$, 33 [states/Ry] in Ni_3AlB, and 75 [states/Ry] in Ni_3Al. Thus there is no room for itinerant ferromagnetism in

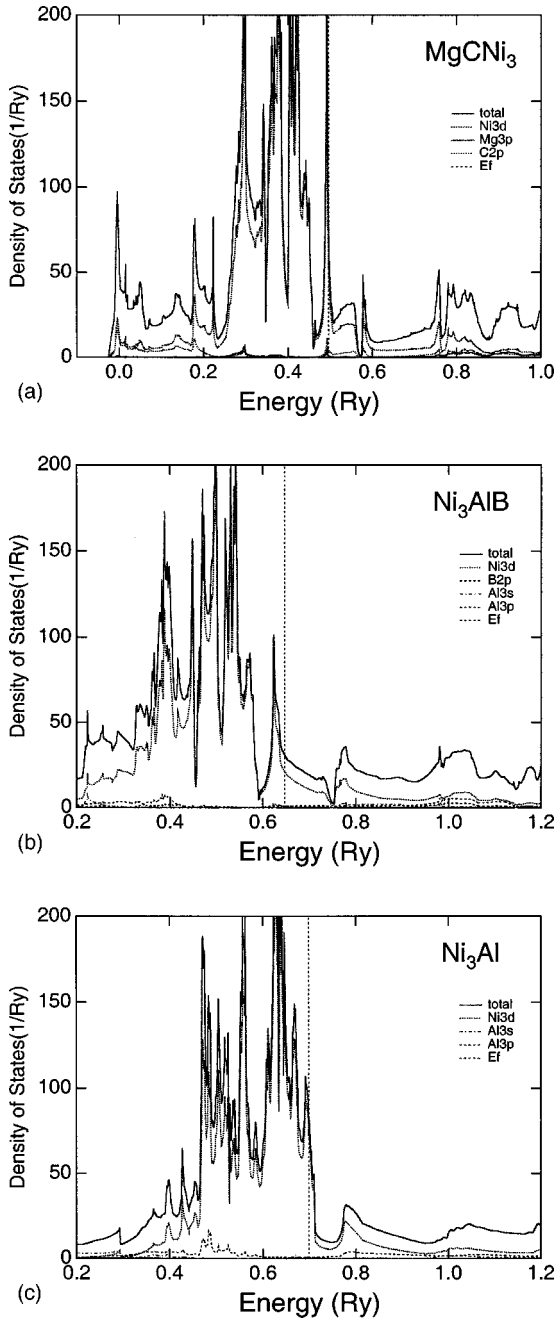

FIG. 2. Density of states (DOS) curve for (a) $MgCNi_3$, (b) Ni_3AlB, and (c) Ni_3Al (in states per Ry and per unit cell). For (a) and (b), Ni-*d* bandwidth is estimated by the two peaks marked by triangles.

Ni_3AlB. The Ni-*d* bands of $MgCNi_3$ and Ni_3AlB are narrow in energy, compared to that of $NiAl_3$, due to the expansion of the lattice and thus due to a decrease of direct Ni–Ni interactions. The shape of the DOS curve closely resembles between Ni_3AlB and $MgCNi_3$. However, since the peak just below the E_F (vHS peak) is higher in $MgCNi_3$, $D(E_F)$ is about twice as high in $MgCNi_3$ compared to Ni_3AlB. We found that the analogous compound Ni_3AlC also has a sharp vHS peak, and its sharpness is comparable to that of $MgCNi_3$.[20] Thus we conclude that the sharpness of the vHS peak is mainly determined by the hybridization between

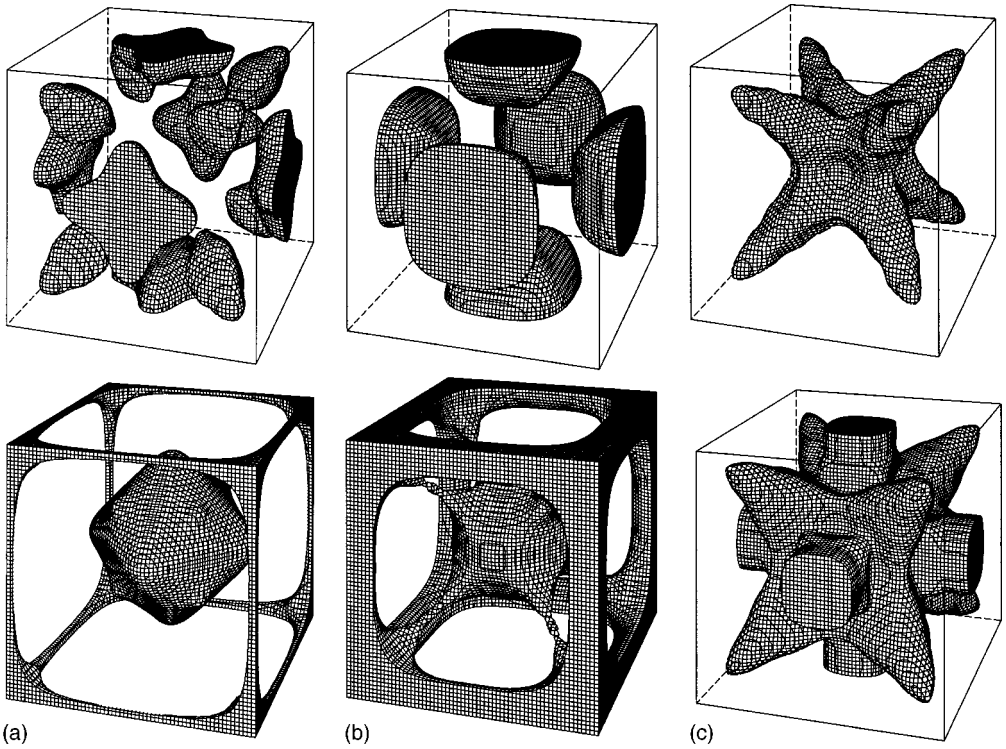

FIG. 3. A perspective view of FSs of (a) $MgCNi_3$, (b) Ni_3AlB, and (c) Ni_3Al. Very small FSs (14th and 15th, which contains 0.001 and 0.002 holes, respectively) are not shown. The center of each cube is the Γ-point.

Ni-*d* and B/C-*p* orbitals. A similar smearing of the vHS peak is also found in $MgBNi_3$.[17] We confirmed that the sharpness of this vHS peak is almost unchanged when the lattice constant *a* in $MgCNi_3$ and Ni_3AlC is contracted by 5%.

The Fermi surfaces (FSs) of $MgCNi_3$, Ni_3AlB, and Ni_3Al are shown in Fig. 3. As is expected by the resemblance of the band structure of $MgCNi_3$ and Ni_3AlB, the FSs also have common features in $MgCNi_3$ and Ni_3AlB. Ni_3Al has definitely different FSs due to the different number of valence electrons and the strong hybridization of Al-*p* orbitals to the main Ni-*d* bands, which is suppressed in $MgCNi_3$ and Ni_3AlB. There are two Fermi surfaces (18th hole and 19th electron bands) in $MgCNi_3$ and Ni_3AlB, and both are predicted to be compensated metals. Each FS contains 0.25 holes and 0.25 electrons in $MgCNi_3$, and 0.40 holes and 0.40 electrons in Ni_3AlB, respectively. There are mainly three differences between the FSs of $MgCNi_3$ and Ni_3AlB: First, the hole band in $MgCNi_3$ has a rather complex shape but that in Ni_3AlB is very simple pill-shaped centered at the *X* points. Second, the "jungle-gym" along the first BZ boundary is thin in $MgCNi_3$ and fat in Ni_3AlB. Finally the DOS of the hole band has 65 [states/Ry] in $MgCNi_3$ and 16 [states/Ry] in Ni_3AlB. This means that the hole FS is quite heavy in $MgCNi_3$ but is light in Ni_3AlB. This is mainly due to the above-mentioned vHS peak, which gives a large DOS and large carrier mass when it is sharp.

A plausible theory which reconciles the two above-mentioned literally inconsistent experimental results (Hebel-Slichter peak in NMR and zero-bias anomaly in tunneling spectra) is presented by Voelker and Sigrist.[21] This theory is essentially a multiband theory first presented by Agterberg.[22] They noticed that $MgCNi_3$ has essentially two Fermi surfaces (FSs), one is the pill-shaped hole FS centered at *X* points, and the other is the electron FS centered at Γ point. The superconducting gap on the warped hole band has an extraordinary "*d*-wave" symmetry, and it competes with the ordinary s-wave-like gap on the electron band. The topology of the FSs used on this model is the same in Ni_3AlB, and thus the same model will be also applicable if Ni_3AlB is superconducting.

Next we consider the electron-phonon interaction in Ni_3AlB. The estimated electron-phonon coupling constant λ_{ph} is 0.67 in $MgBNi_3$ and 1.36 in $MgCNi_3$, assuming a Debye temperature $\Theta_D = 300$K.[17] This value crucially depends on the Debye temperature Θ_D and may give an upper bound to λ_{ph}. If we just substitute $D(E_F)$ for Ni_3AlB and use the McMillan formula one would obtain $\lambda_{ph} = 0.33$ and $T_c = 0.07$ K. If, however, hole doping is possible and E_F is just on the vHS peak, we obtain $D(E_F) = 99.4$ [states/Ry], $\lambda_{ph} = 1.02$ and $T_c = 15$ K. Such hole doping may be possible by Mg substitution for Al, and/or off-stoichiometry of B. Note that in $MgBNi_3$, E_F already settles on the vHS peak and further increase of $D(E_F)$ is not expected by small carrier doping.[17] In $MgCNi_3$, due to the strong ferromagnetic spin fluctuation, T_c is depressed significantly.[9] In the case of Ni_3AlB, due to stronger hybridization of B-*p* orbitals, spin fluctuations will be suppressed and a higher T_c can be expected.

Finally we discuss the formation energy of Ni_3AlB. Ni_3AlB_x is synthesized so far only below $x \sim 0.15$ using conventional solid-state reaction method.[10] We estimate the formation energy of Ni_3Al and Ni_3AlB as the following equations:

$$E(\mathrm{Ni_3Al}) = 3E(\mathrm{Ni}) + E(\mathrm{Al}) + \Delta E_1,$$

$$E(\mathrm{Ni_3AlB}) = 3E(\mathrm{Ni}) + E(\mathrm{Al}) + E(\mathrm{B}) + \Delta E_2$$
$$= E(\mathrm{Ni_3Al}) + E(\mathrm{B}) + \Delta E_3,$$

where $E(\mathrm{A})$ denotes the total energy of A-compound per formula unit obtained by this *ab initio* calculation.[23] We obtain

$$\Delta E_1 = -0.121\ \mathrm{Ry/atom} = -38\ \mathrm{kcal/mol},$$

$$\Delta E_2 = -0.098\ \mathrm{Ry/atom} = -31\ \mathrm{kcal/mol},$$

$$\Delta E_3 = +0.023\ \mathrm{Ry/atom} = +7.2\ \mathrm{kcal/mol}.$$

The value of ΔE_1 is in good agreement with previous calculation.[18] We see that Ni_3AlB is much more stable than Ni+Al+B, but slightly less stable than Ni_3Al+B. Nevertheless, it is possible that Ni_3AlB is in a metastable state. Even if Ni_3AlB itself cannot be synthesized, it may be possible to synthesize Ni_3AlB_x with more boron content x than was synthesized so far. In that case, our discussions above may also be applicable.

In summary, the electronic energy band structure has been calculated for $MgCNi_3$, Ni_3AlB, and Ni_3Al by the FLAPW method within LDA. Due to the strong hybridization between Ni-*d* and B-*p* orbitals, the shape of Fermi surfaces of Ni_3AlB is quite different from that of Ni_3Al. The shape and topology of the FSs of Ni_3AlB resemble those of $MgCNi_3$, while $D(E_F)$ of Ni_3AlB is about half that of $MgCNi_3$.

We thank T. Kanomata and K. Koyama for giving us unpublished work and for enlightening discussions. Numerical computation was mainly performed at the Tsukuba Advanced Computing Center at the Agency of Industrial Science and Technology.

*Electronic address: i.hase@aist.go.jp

[1] T. He, Q. Huang, A. P. Ramire, Y. Wang, K. A. Rega, N. Rogado, M. A. Hayward, M. K. Haas, J. S. Slusky, K. Inumara, H. W. Zandbergen, N. P. Ong, and R. J. Cava, Nature (London) **411**, 54 (2001).

[2] C. Pfiderer, M. Uhlarz, S. M. Hayden, R. Vollmer, H. von Lohneysen, N. R. Bernhoeft, and G. G. Lonzarich, Nature (London) **412**, 58 (2001).

[3] S. S. Saxena, P. Agarwal, K. Ahilan, F. M. Grosche, R. K. W. Haselwimmer, N. J. Steiner, E. Pugh, I. R. Walker, S. R. Julian, P. Monthoux, G. G. Lonzarich, A. Huxley, I. Sheikin, C. Braithwaite, and J. Flouquet, Nature (London) **406**, 587 (2000).

[4] Y. Maeno, H. Hashimoto, K. Yoshida, S. Nishizaki, T. Fujita, J. G. Bednorz, and F. Lichtenberg, Nature (London) **372**, 572 (1994).

[5] H. Rosner, R. Weht, M. D. Johannes, W. E. Pickett, and E. Tosatti, Phys. Rev. Lett. **88**, 027001 (2002).

[6] Z. Q. Mao, M. M. Rosario, K. D. Nelson, K. Wu, I. G. Deac, P. Schiffer, Y. Liu, T. He, K. A. Regan, and R. J. Cava, Phys. Rev. B **67**, 094502 (2003).

[7] G. Kinoda, M. Nishiyama, Y. Zhao, M. Murakami, N. Koshizuka, and T. Hasegawa, Jpn. J. Appl. Phys., Part 2 **40**, L1365 (2001).

[8] P. M. Singer, T. Imai, T. He, M. A. Hayward, and R. J. Cava, Phys. Rev. Lett. **87**, 257601 (2001).

[9] D. J. Singh and I. I. Mazin, Phys. Rev. B **64**, 140507(R) (2001).

[10] T. Kanomata (unpublished).

[11] A. Yanase, *Fortran Program For Space Group (TSPACE)* (in Japanese) (Shokabo, Tokyo, 1995).

[12] O. Gunnarson and B. I. Lundqvist, Phys. Rev. B **13**, 4274 (1976).

[13] J. H. Xu, B. I. Min, A. J. Freeman, and T. Oguchi, Phys. Rev. B **41**, 5010 (1990), and references therein.

[14] G. Y. Guo, Y. K. Wang, and L. S. Hsu, J. Magn. Magn. Mater. **239**, 91 (2002).

[15] M. A. Hayward, M. K. Haas, A. P. Ramirez, T. He, K. A. Regan, N. Rogado, K. Inumaru, and R. J. Cava, Solid State Commun. **119**, 491 (2001).

[16] S. B. Dugdale and T. Jarlborg, Phys. Rev. B **64**, 100508(R) (2001).

[17] J. H. Shim, S. K. Kwon, and B. I. Min, Phys. Rev. B **64**, 180510(R) (2001).

[18] B. I. Min, A. J. Freeman, and H. J. F. Jansen, Phys. Rev. B **37**, 6757 (1988).

[19] S. N. Sun, N. Kioussis, S. P. Lim, A. Gonis, and W. H. Gourdin, Phys. Rev. B **52**, 14 421 (1995).

[20] I. Hase (unpublished).

[21] K. Voelker and M. Sigrist, cond-mat/0208367.

[22] D. F. Agterberg, V. Barzykin, and L. P. Gor'kov, Phys. Rev. B **60**, 14 868 (1999); Europhys. Lett. **48**, 449 (1999).

[23] We used the experimental lattice constants for the total-energy calculation of α-B, fcc-Al, fcc-Ni, and Ni_3Al. For Ni_3AlB we used the optimized lattice constant $a = 3.765$ Å. The convergence of the total energy for the change of parameters ($K_{\max}$, and the number of **k**-points) are ~10 mRy per formula unit.